





RESEARCH ARTICLE | JULY 16 2024

OPTEMIST: A neutral beam for measuring quasi-omnigenity in Wendelstein 7-X

Samuel A. Lazerson ; David Kulla ; Paul McNeely; Norbert Rust; Lucas van Ham ; Dirk Hartmann ; W7-X Team



Phys. Plasmas 31, 072506 (2024)

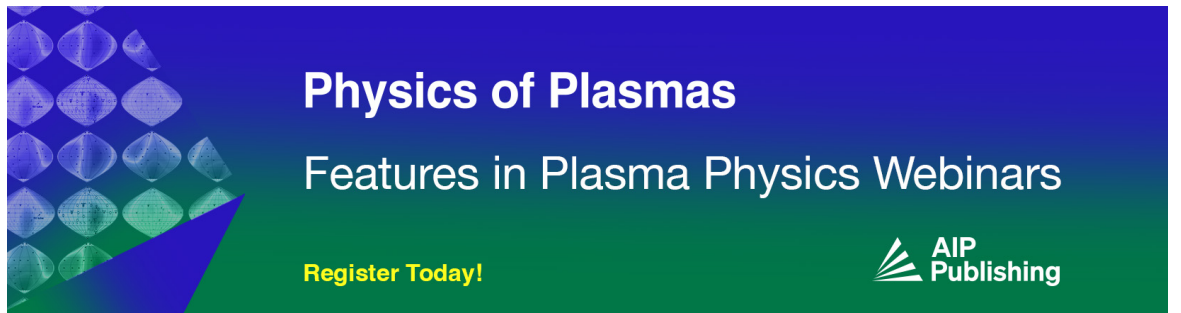
<https://doi.org/10.1063/5.0218670>



View Online




Export Citation



Physics of Plasmas
Features in Plasma Physics Webinars

Register Today!



OPTEMIST: A neutral beam for measuring quasi-omnigenity in Wendelstein 7-X

Cite as: Phys. Plasmas **31**, 072506 (2024); doi: [10.1063/5.0218670](https://doi.org/10.1063/5.0218670)

Submitted: 13 May 2024 · Accepted: 25 June 2024 ·

Published Online: 16 July 2024



View Online



Export Citation



CrossMark

Samuel A. Lazerson,^{1,a)} David Kulla,² Paul McNeely,¹ Norbert Rust,¹ Lucas van Ham,¹ Dirk Hartmann,¹
and W7-X Team^{b)}

AFFILIATIONS

¹Max-Planck-Institut für Plasmaphysik, Greifswald 17491, Germany

²Max-Planck-Institut für Plasmaphysik, Garching bei München 85748, Germany

^{a)}Author to whom correspondence should be addressed: samuel.lazerson@ipp.mpg.de

^{b)}See Thomas Sunn Pedersen *et al.*, Nucl. Fusion **62**, 042022 (2020) for the full list of W7-X team members.

ABSTRACT

A new neutral beamline (OPTEMIST) uniquely capable of exploring the predicted improvement of fast ion confinement in Wendelstein 7-X (W7-X), which comes with increasing plasma beta, is proposed. As the plasma beta increases in the W7-X device, the high mirror magnetic configuration has drift orbits that begin to close, enhancing the confinement of the deeply trapped particles. The existing neutral beam system is found to produce particle populations that do not adequately probe the deeply trapped orbits. Fast tritons generated by thermal deuterium–deuterium fusion reactions are found to probe the necessary conditions for demonstrating this effect. However, it is found that diagnostically measuring this effect will be difficult. A scoping study of a neutral beamline that directly populates the trapped orbits is performed. It is found that a monoenergetic population of 120 kV injected protons provides the largest confinement enhancement in the fast ion population as the plasma beta is increased. The necessity to raise plasma density to increase plasma beta results in blinding of spectroscopic beam measurements by bremsstrahlung. An array of novel fast ion loss detectors that would adequately assess the confinement of these particles is proposed.

© 2024 Author(s). All article content, except where otherwise noted, is licensed under a Creative Commons Attribution (CC BY) license (<https://creativecommons.org/licenses/by/4.0/>). <https://doi.org/10.1063/5.0218670>

I. INTRODUCTION

The Wendelstein 7-X (W7-X) experiment is predicted to have a fast ion confinement of deeply trapped particles, which improves with plasma beta, attributed to the quasi-omnigenous (QO) nature of the device.^{1,2} In W7-X, the poloidal variation of the magnetic field strength is significantly less than that in the toroidal direction (Fig. 1). This gives the device a toroidal mirror like character, especially in the high mirror magnetic configuration. Deeply trapped particles will mirror between the regions of high field, located in the bean-shaped cross section, while precessing in the poloidal direction. In W7-X, the poloidal precession is driven predominantly by $\vec{E} \times \vec{B}$, while in other devices it can be driven by the magnetic drifts alone.³ Generally, at low plasma beta these deeply trapped particles experience a net radially outward drift (due to curvature drift terms) and are lost from the plasma. As plasma beta increases, the drift surfaces for these particles begin to form closed surfaces, implying that these particles become better confined.⁴ In this work, we assess the ability of existing fast ion sources (and diagnostics) to demonstrate and probe this effect and propose a

new system and diagnostic set uniquely tuned to assessing this character.

In order to probe the QO nature of fast ions in W7-X, there are some necessary conditions the fast ions must fulfill. The most obvious of them is that they be born and remain trapped. This condition implies geometric constraints on their generation: that their energy at birth be mostly in the perpendicular direction and that they be born at or near the low field section (triangular cross section of the plasma). Note that the field at which a particle mirrors is defined as $\vec{B}_{\text{mirror}} = \vec{B}_{\text{birth}}(1 + v_{\parallel}^2/v_{\text{perp}}^2)$ and that the toroidal variation of magnetic field is approximately 15%. This implies that small amounts of parallel velocity are sufficient to create passing particles even when particles are born at the minimum of the magnetic field (the W7-X triangular cross section). Second, the particles must be collisionless, as large pitch angle scattering collisions will essentially randomize the orbits. In general, this can be avoided by keeping the particle energy well above the so-called critical energy (below which pitch angle scattering dominates particle orbits). The critical energy can be simply written in terms of

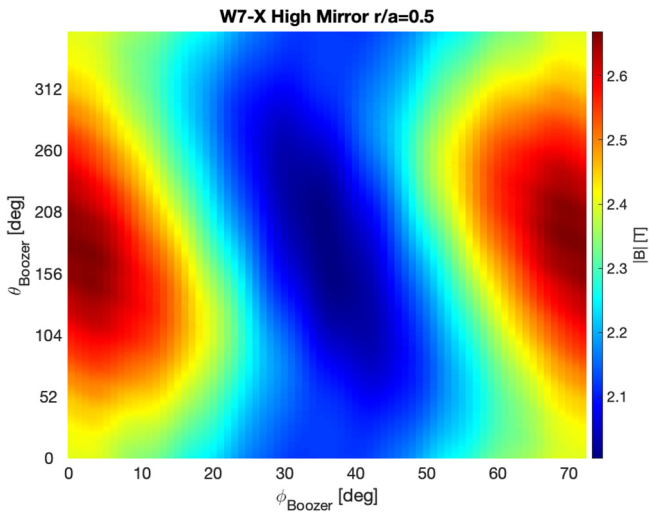


FIG. 1. Contours of $|\vec{B}|$ in a given W7-X field period, indicating the toroidal and poloidal nature of the field.

the plasma particle mass, fast ion mass, and the electron temperature ($E_{\text{crit}} = 14.8 \frac{A_{\text{fast}}}{A_{\text{plasma}}^{2/3}} T_e$, where A is the effective ion mass and T_e is the electron temperature in energy units). For W7-X, electron temperatures lie in the 1–4 keV range, suggesting a critical energy of around 15–60 keV in hydrogen. Related to these two conditions is the additional consideration that mode activity does not play a strong role in the radial motion of the particles. Generally, W7-X discharges are quiescent as the NBI system on W7-X does not generate a large enough fast ion population to destabilize Alfvénic modes.⁵ In summary, to probe the QO nature of W7-X, deeply trapped particle at energies above 60 keV must be generated.

The W7-X device has three methods of generating fast ions: neutral beam injection (NBI),⁶ ion-cyclotron resonance heating (ICRH),⁷

and deuterium–deuterium fusion births. It has already been established that neutral beam injected particles do not show an improvement in fast ion confinement with beta.⁸ It will be shown in detail in this work that this is because the neutral beam injected ions fulfill neither of the criteria for measuring the QO nature of W7-X. This however makes them excellent heating beams despite their non-tangential injection geometry. Under its nominal configuration, the ICRH system has a resonance in the bean-shaped cross section where fields are highest. This configuration in W7-X is similar to the high field side launch envisioned for tokamaks. The antenna may be phased such that the resonance lies in the triangular cross section, the details of which are left to a separate work. However, generation of particles with sufficient energy is questionable without invoking a three-ion scheme.⁹ Moreover, ICRH accelerates particles by kicks in energy similar to those of pitch angle scattering, bringing into question how randomized the high energy particle orbits become while ICRH is on. The third method of fast ion generation is from fusion products during deuterium operation. This produces small, but measurable, fast triton and proton populations. However, the high energy of these particles may violate the small gyro-radius approximation at 2.5T necessary to invoke the drift orbit approximation. It appears that existing methods for generating fast ions may be insufficient for demonstrating the QO nature of W7-X fast ion confinement, motivating the exploration of a new fast ion generation system.

In this work, we provide a physics basis and diagnostic scoping for OPTEMIST (Omnigeneous Particle Test EMISsion in Triangular cross section), a new neutral beam for demonstrating the QO nature of W7-X fast ion orbits (Fig. 2). In Sec. II, we describe the tools used in this assessment, general geometry of our proposed new system, and profiles/equilibria used for our scan in beta. In Sec. III, we discuss our results focusing on the behavior of the existing NBI system, the behavior for fusion born products, the behavior of the OPTEMIST beam, and a general scoping study of various diagnostics for assessing the OPTEMIST results. Finally, in Sec. IV we discuss the feasibility of the OPTEMIST beamline, challenges in its development, and future work.

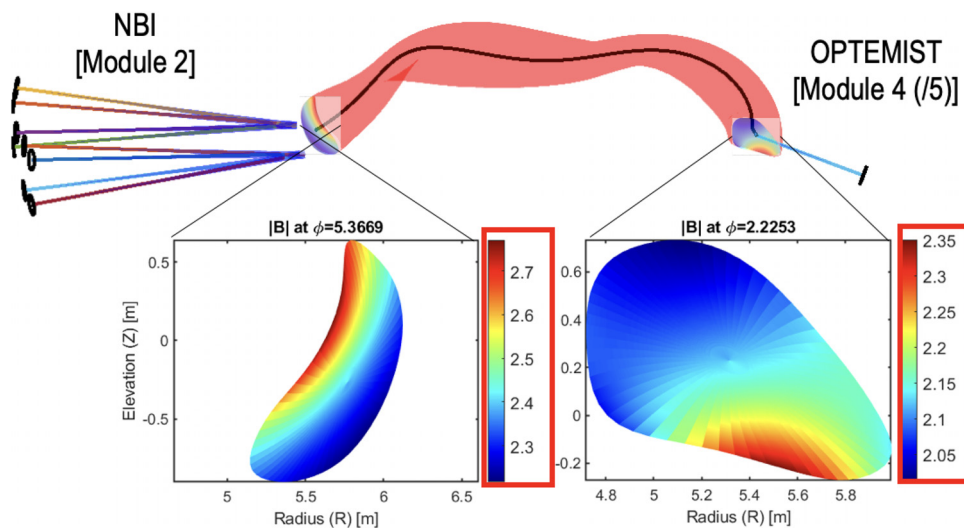


FIG. 2. Depiction of the existing W7-X neutral beamlines and the proposed OPTEMIST beamline. OPTEMIST clearly injects into regions of much lower magnetic field.

24 July 2024 06:56:36

II. METHOD

In this work, we explore neutral beam injected and fusion born products with the BEAMS3D and FIDASIM codes.^{10,11} The BEAMS3D code is a Monte Carlo neutral beam injection and Fokker-Planck solver code capable of following particles in both gyro-center and gyro-orbit modes.¹² The code takes a variety of magnetic field models including VMEC equilibria,¹³ is capable of following particles to detailed wall models based on CAD data, and has recently been interfaced to the FIDASIM code providing synthetic diagnostics for both fast ion D-alpha (FIDA) and neutral particle analyzers (NPAs).¹⁴ The FIDASIM capability builds on work validating the BEAMS3D fast ion model against experiment data in ASDEX-U. A beta scan is performed using VMEC equilibria with self-consistent plasma profiles. Neoclassical calculations provide estimates for both toroidal current density and the radial electric field. Simulations are performed for the existing neutral beam system on W7-X, D-D fusion products and the proposed OPTEMIST beamline.

Neutral beam injection is modeled using the Suzuki model for hydrogenic species.¹⁵ Here, VMEC provides the mapping from flux space to cylindrical space for both magnetic and kinetic quantities (temperatures and densities). For the W7-X neutral beamline, the detailed port model is considered.¹⁶ Simulations of fusion births are performed using the Bosch and Hale model for D-D fusion reactions.^{17,18} Fast ions are followed on a cylindrical grid with either gyro-center or full-orbit models as appropriate.^{12,19} Pitch angle scattering and collisional operators are included in the simulations. The background grid extends in the cylindrical dimensions from $R = [4.25, 6.5] m$, $\phi = [0.0, 72]^\circ$, $Z = [-1.25, 1.25] m$ with 128, 72, and 128 grid points, respectively. For more details of the code, the interested reader should consult previous publications.

In order to simulate the diagnostic response of the FIDA and NPA diagnostics for the OPTEMIST beamline, a newly developed interface between FIDASIM and BEAMS3D is leveraged. The FIDASIM code provides a means of solving the complex collisional-radiative problem of the calculation of light emitted by charge exchange reactions between neutral beam species and various plasma populations. In particular, we are interested in spectra produced by

interactions of the neutral beam and background plasma (beam emission) and those between the neutral beam and fast ion population (FIDA). It is traditional to use the ratio of these two signals as a measure of changes in fast ion confinement. Additionally, the measurement of escaping neutrals generated through charge exchange processes (between neutral beam and fast ions) is modeled by FIDASIM. As only the OPTEMIST beam is found as a feasible source for measuring the QO nature of fast ions in W7-X, we restrict its use to those simulations. Additionally, full orbit simulations to the first wall provide locations for measurement of lost fast ions by wall tiles instrumented with Faraday cup fast ion loss detectors.^{8,20,21}

As the effect of improved fast ion confinement is a function of plasma beta, a set of VMEC equilibria with self-consistent profiles is generated for this work. In these simulations, model profiles that are a good approximation to plasma parameters achievable in steady state W7-X discharges are used. The electron temperature profile is modeled as being linear in $r/a = \rho = \sqrt{s}$ where s is the usual normalized toroidal flux ($T_e(\rho) = (T_{e0} - T_{e-edge})(1 - \rho) + T_{e-edge}$, where T_{e0} and T_{e-edge} are the core and edge electron temperatures, respectively). The ion temperature is taken equal to the electron temperature with a maximum temperature of 1.5 keV to mimic the ion temperature clamping seen in W7-X discharges. The electron density is taken to be $n_e(\rho) = n_{e0}$, where n_{e0} is the core electron density. For this work, the effect of impurities is ignored and the ion density is taken to be equal to the electron density. Sample profiles can be seen in Fig. 3. The pressure profile is then constructed to be self-consistent with the kinetic profiles. Neoclassical quantities (bootstrap and the radial electric field) are calculated using the NEOTRANSP code, which is based on precomputed DKES simulations for the W7-X high mirror magnetic configuration.²²

The proposed OPTEMIST beamline can be seen in Fig. 4. This port was originally intended for a diagnostic neutral beam, which was never installed. The beam model itself is a point source with similar divergence to that of the existing neutral beamlines. In the FIDASIM simulations, an array of ports is chosen each with 64 channels scanning through the beam path across the plasma. This is done to help provide a large set of diagnostic sight lines from which one could downselect. This applies for NPA and FIDA diagnostics.

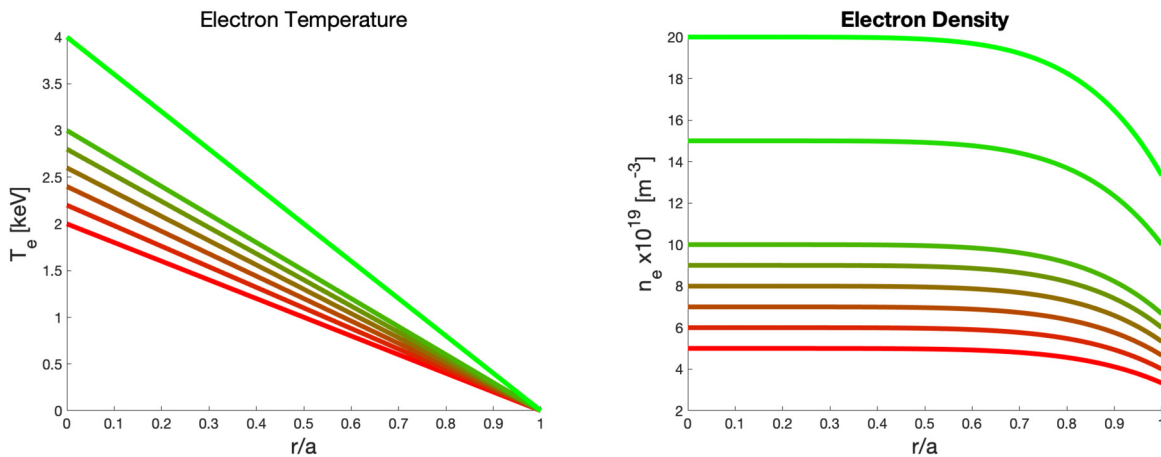


FIG. 3. Electron temperature (left) and density profiles (right) scanning beta used in this work. Ion temperatures are set equal to the electron temperature with a 1.6 keV max temperature.

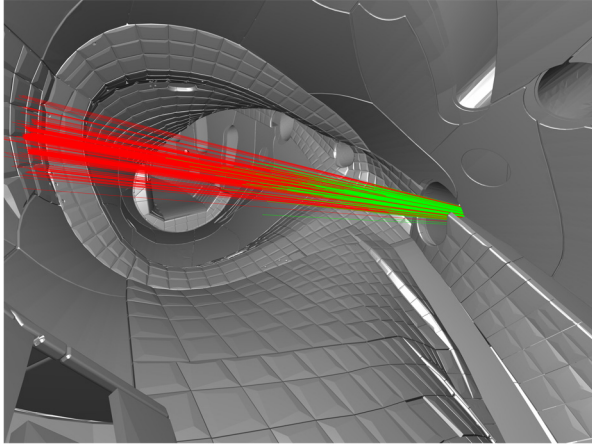


FIG. 4. OPTEMIST geometry showing the W7-X first wall. Red traces show shine-through particles while green are those that ionize in the plasma.

III. RESULTS

A. The W7-X neutral beam system

The confinement of neutral beam produced fast ions is investigated via BEAMS3D simulations across multiple plasma beta scenarios. We find the injection geometry generally produces passing particles. This implies that one of the necessary conditions for study to the QO nature of W7-X is not met. Collisional simulations of the confinement of these fast ions shows a highly collisional picture with no apparent improvement in confinement with increasing beta. However, this does highlight the value of this system as a heating tool. Finally, while losses do show some toroidal asymmetry, a significant number of particles are lost in all modules of the machine. This suggests passing particles are being randomly trapped and lost promptly. Overall, the neutral beam system is found to be a poor source of fast ions for probing the QO nature of W7-X.

In Fig. 5, we depict the birth distribution for sources 7 and 8 in the mirror magnetic field space. In this figure, we depict the poloidal variation of magnetic field in the bean (red) and triangular (blue) cross sections. For a particle to be born trapped, it must be born to the left of the red region. We can see that at 0.5% and 2.7% plasma beta, the neutral beam sources inject particle onto passing orbits, with the more toroidal orientation of source 8 generating strongly passing particles. The energy fractions are plotted to show that in W7-X the orbits are strictly a function of geometry and not energy. It should be noted that the mirror image sources 3 and 4 will have the exact same distribution. Sources 1, 2, 5, and 6 are yet to be installed but simply move the sources in the vertical direction, making little difference to the birth distribution. The W7-X neutral beam system simply does not populate trapped orbits in the high mirror magnetic configuration.

One may ask if a more radial injection geometry at the NBI port location could change the situation. While this will reduce the parallel velocity of the particles at birth, we find that this biases the beam toward injection at even higher magnetic field (points the beam toward the bean-shaped cross section). This may produce some trapped particles but at such a high magnetic field that they cannot be considered deeply trapped. Deeply trapped particles are the ones we wish to show have improved confinement with plasma beta.

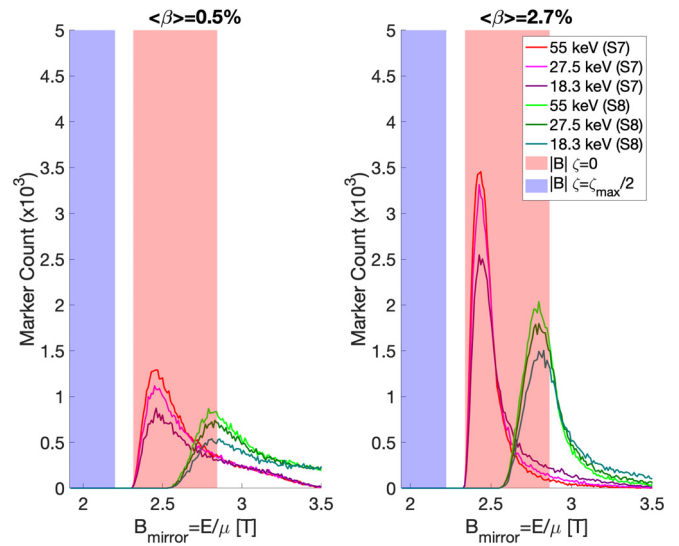


FIG. 5. The mirror magnetic field is shown for the birth distribution of particles in W7-X high mirror magnetic configuration at 0.5% and 2.7% plasma beta. The red shaded region indicates the poloidal variation in magnetic field in the bean-shaped cross section and the blue region indicates the poloidal variation in field strength in the triangular cross sections.

The plasma density along with a strongly passing particle fast ion population play a large role in slowing down simulations (Fig. 6). While we saw an increase in fast ion births with increasing density (plasma beta), we see a general decrease in the fast ion density. This is associated with the effect of collisions increasing with density, thereby reducing the time of flight for a given confined particle. For this reason, the fast ion density should be normalized to the birth profile to provide a better sense of confinement. In this case, doing so only makes the picture worse, further reducing the normalized fast ion density with increasing beta. Looking at the toroidal symmetry of the fast ion distribution function, we see no clear toroidal asymmetry. This points to a purely passing population contributing to the fast ion density.

The fraction of born particles that are lost shows a general decrease in confinement with increasing plasma beta (Fig. 7). The general degradation in confinement for the neutral beam injected particles has been reported elsewhere.⁸ The points below 1.5% plasma beta scan density and temperature in step. Density rises from 5×10^{19} to $10 \times 10^{19} \text{ m}^{-3}$, while the electron temperature rises from 2 to 3 keV. This implies a relatively small change in critical energy and thus collisionality regime for the particles. The two higher beta configurations are evaluated at 4 keV electron temperature. The increased losses from these configurations are associated with a more collisional plasma for the NBI fast ions and thus greater pitch angle scattering.

Overall, the neutral beam system on W7-X lacks the correct toroidal geometry to populate trapped orbits and possesses an injection energy that is too collisional to assess collisionless orbits. While this makes the system a poor choice for assessing the QO nature of W7-X, it does allow the beam to effectively heat despite a rather unattractive injection geometry. What can be learned from this exercise in assessment of the W7-X neutral beam system is that assessment of the QO nature with neutral beam injection requires a neutral beam located

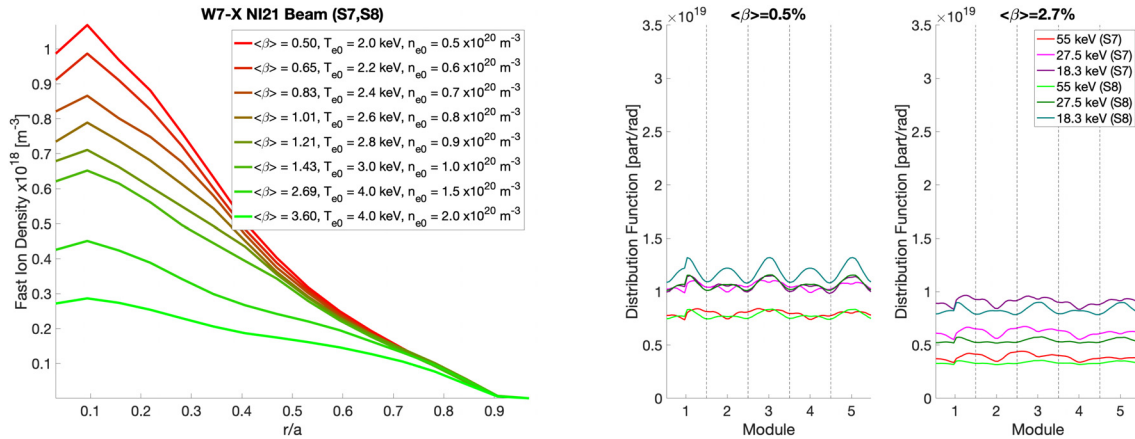


FIG. 6. The radial (left) and toroidal (right) fast ion distribution for sources 7 and 8. A decrease in fast ion distribution with increasing beta is attributed to the increasing density, while lack of toroidal asymmetry between modules highlights the lack of toroidally trapped particles.

more toroidally toward the triangular cross section and at high injection energy.

B. Fusion products

The fusion of thermal deuterium species produces an isotropic distribution of fast ions whose confinement was investigated with the gyro-orbit capability of the BEAMS3D code.¹² The isotropic nature of thermal fusion births implies that some particles will be born deeply trapped, while energies are large enough to be in the collisionless regime. In this analysis, we focus on the confinement of the 1 MeV triton production as it has the lowest overall particle velocity of the three possible reaction products (protons, tritons, $^3\text{He}^{+2}$). However, it should be noted that both the fast protons and tritons have gyro-radii of approximately 10 cm (with the $^3\text{He}^{+2}$ being approximately 5 cm).

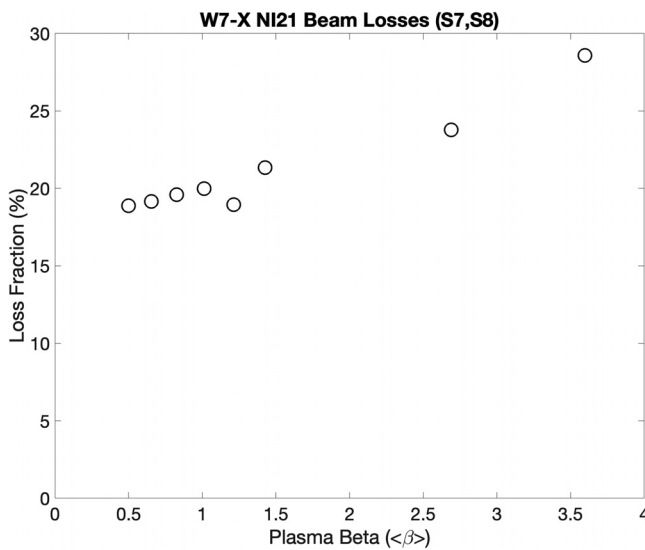


FIG. 7. Neutral beam losses from sources 7 and 8 showing a general degradation in confinement.

Thus, these particles may not be well suited to the study of QO fast ion confinement given the breakdown of the gyro-center approximation at the nominal 2.5 T W7-X field. Additionally, we ignore the $^3\text{He}^{+2}$ ions as their birthrate is significantly lower than that of fast protons and tritons. The overall confinement of D-D produced fast tritons was covered in a previous work.²³

The birth of thermal fusion products is isotropic in pitch angle space, so a subset of particles will be born deeply trapped in every field period of W7-X. This provides one of the two necessary conditions for the study of such particles in W7-X. The second condition is met by the high energy of these particles. The challenge is to measure the confinement of these particles, specifically to distinguish their confinement from the overall confinement of the entire fast ion population. One may assume that the majority of passing particles are well confined and so measurements of particle loss with low pitch angle predominantly measure particles born trapped.

Figure 8 depicts the loss of trapped fast tritons produced by D-D thermal particle fusion in W7-X. For timescales on the order of milliseconds, we find that confinement improves with increasing plasma beta. However, we note that the overall confinement on longer timescales shows only a small improvement with plasma beta. Such a small improvement would most likely be indistinguishable diagnostically. Shorter timescales, associated with prompt losses, shows a slight increase in losses with plasma beta.

An additional complication that arises from the use of fusion products as a fast ion source is that their birthrate is a strong function of the plasma parameters. This means that as plasma beta increases, the number of particles generated is increased. While this is true for neutral beam measurements as well, the relative change in fast ion content can still be calculated by normalizing to the emissions from beam deposition. Unfortunately, a direct measurement of fusion product births is quite challenging. Here, one may be able to normalize to the measurement of neutron rates. Figure 9 attempts to show this by normalizing the poloidal distribution of deeply trapped losses to the total number of fast ions born. We clearly see a decrease in losses for certain positions while losses increase at other positions. Losses for fast tritons are toroidally localized to the module in which deeply trapped particles are born. Thus, an array of Faraday cup fast ion loss detectors (FC-

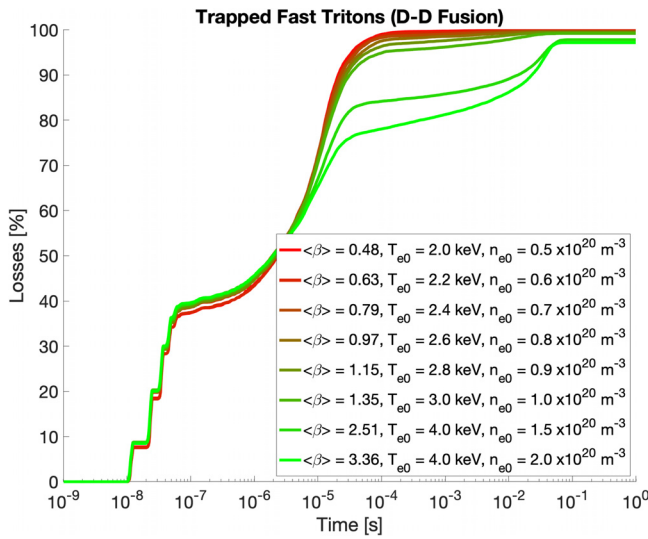


FIG. 8. Temporal loss evolution of trapped fast tritons in W7-X. Trapping is defined as particles with a mirror magnetic field less than the minimum magnetic field in the bean-shaped cross section.

FILDs) coupled with neutron diagnostics may be able to discern this feature. Finally, we note that studies of fast ion confinement changes due to neutral beam power variation in the Large Helical Device did make use of neutron measurements as a proxy for fast ion confinement.²⁴

C. OPTEMIST

The OPTEMIST beamline is investigated with BEAMS3D code, validating the generation of fast trapped protons, scoping the necessary

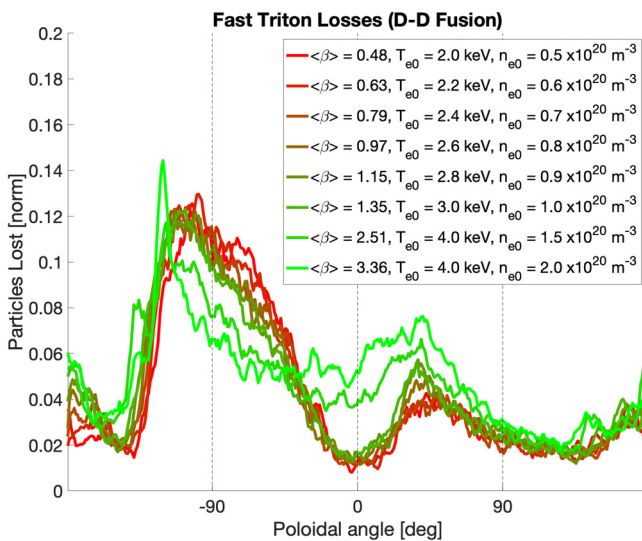


FIG. 9. Poloidal loss structure of deeply trapped fast tritons in W7-X. Losses have been normalized to the total number of fast tritons generated, a proxy for neutron rates. The $\theta = 0^\circ$ position indicates the outboard mid-plane with positive indicating the top of the machine.

beam energy for populating collisionless orbits and demonstrating that the confinement of the trapped population improves with plasma beta. The nearly radial injection of the beam and injection into the triangular cross section (low field region) biases the beam toward the generation of trapped particles. Thus, by construction the beam should fulfill one of our necessary conditions: generation of deeply trapped particles. The simulations of beam energies ranging from 50 to 250 keV are scanned to determine the energy at which the fast ions become sufficiently collisionless, our second necessary condition for the assessment of fast ion confinement in the high mirror magnetic configuration. Finally, we present a preliminary scoping of the ability to measure these changes via beam emission (FIDA) and neutral emission (NPA) using the FIDASIM code. A scoping of the OPTEMIST beamline to measure the QO nature of the high mirror magnetic field using fast ions is presented.

The OPTEMIST beamline, by geometric construction, generates trapped particles as we see in Fig. 10. The beam clearly injects particles into the trapped region, irrespective of energy or plasma beta. In fact, we see that the deposition becomes more deeply trapped as beta increases. An increase in overall amplitude with beta can be attributed to the increase in plasma density associated with the increased plasma beta. There is a reduction in overall deposition with increasing beam energy. This is due to the relatively short path length through the plasma resulting in rather high shine-through. The OPTEMIST beam clearly fulfills the necessary condition of generating deeply trapped particles in W7-X across a wide range of beam and plasma parameters.

The confinement of fast ions injected by the OPTEMIST beam can be seen to improve with plasma beta in Fig. 11. At 50 keV, we clearly see the effect of particles born near the critical energy, with confinement decreasing for increasing plasma beta. This is associated with pitch angle scattering dominating the orbit dynamics. For beam energies greater than 100 keV, the fast ion confinement is found to improve

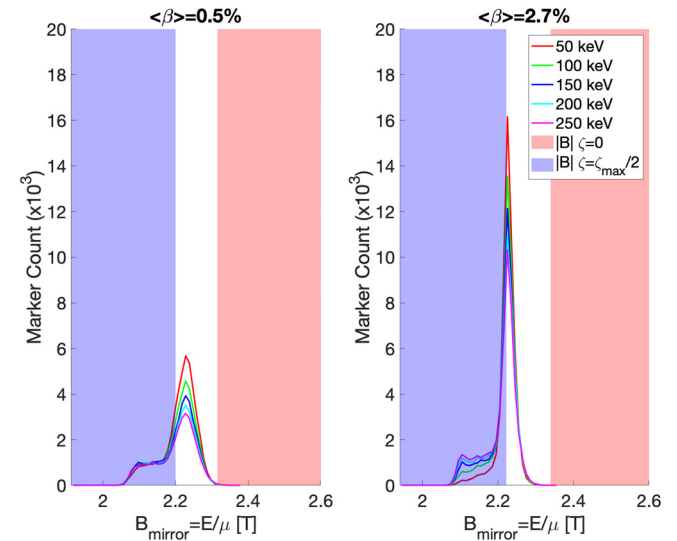


FIG. 10. Mirror magnetic field for particle injected by the OPTEMIST beamline at multiple beam energies and plasma betas, showing generation of trapped particles. The red shaded region indicates the poloidal variation of the magnetic field in the bean-shaped cross section. Particles born to the left of this region are born trapped.

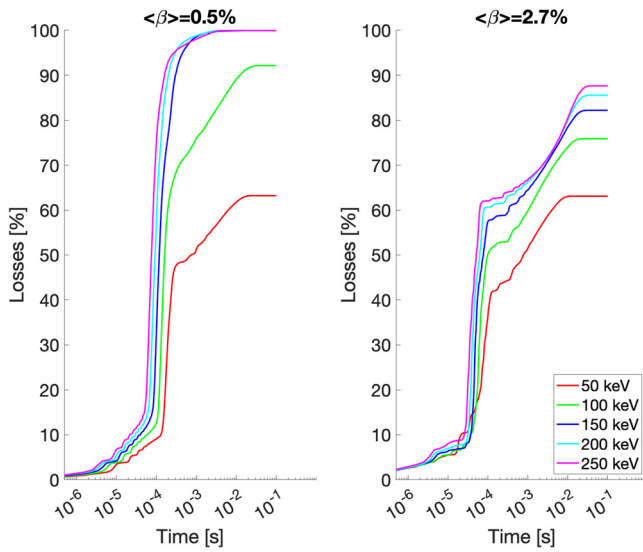


FIG. 11. Fast ion losses for the OPTEMIST beamline at two plasma betas and multiple beam energies. A clear improvement in confinement is seen for energies above 100 keV.

with plasma beta. However, we note that above 100 keV we find 100% loss of fast ions at low plasma beta. We also note that the asymptotic steady-state time for the beam losses appears to be around 100 ms, suggesting short pulse lengths can be sufficient for generating a fast ion distribution. Finally, we see that the greatest change with plasma beta occurs for a 100 keV beam. This suggests that 100 keV may be the desired population to inject and measure. A more detailed scan shows that the difference in confinement peaks for a 120 keV beam with confinement improving by almost 20%.

Simulations of the emitted spectra were performed with the FIDASIM code to scope possible diagnostic geometries and beam power (Fig. 12). A significant challenge to measuring FIDA in W7-X at finite beta comes from bremsstrahlung. This is because W7-X

achieves high beta through high core densities ($n_{e0} > 10^{20} \text{ m}^{-3}$) and modest levels of temperature ($T_{e0} \sim 4 \text{ keV}$). Ignoring the bremsstrahlung, we do find that ratio of the FIDA signal to the beam emission signal (commonly known as FIDA/BES) does increase with increasing beta. While many positions of the diagnostic were considered, all suffer from bremsstrahlung blinding us to the FIDA signal.

It should also be noted here that in most diagnostic scenarios, FIDA light is not generated by the same beam that is generating the fast ion population. Usually, a beamline not in the line of sight of the FIDA optics is used to generate a fast ion population. A second beamline is used to probe the distribution allowing for background subtraction. This, of course, could be avoided if the FIDA signal was well separated from the beam emission signal and very strong, an unlikely scenario. A scan of power from 1 MW ($\sim 8 \text{ A}$) to 8 MW ($\sim 70 \text{ A}$) was performed of the monoenergetic 120 keV beam to see if with enough power a strong enough signal could be emitted. While signal levels did increase, the FIDA signal never became significant relative to the bremsstrahlung. Even so, a limited optical system viewing the beam could provide measurements of the beam emission (deposition).

A preliminary study on neutral particle analyzer synthetic signals using FIDASIM was also performed. Similar viewing geometries as those considered for the FIDA studies were considered. In general, the neutral flux around 120 keV was not found to increase as the beta value went from $\sim 0.5\%$ to $\sim 1.5\%$ beta but actually decreased as the beta value increased further. Normalizing this signal to the beam emission signal as is done with FIDA, did lead to recovery of a continual increase in signal with plasma beta. Passive neutral emission was not considered in this work. Previous works would suggest passive neutrals for this system would not pollute the low beta signal.²⁵ However, such estimates at high beta (high density) may no longer hold as neutral densities may significantly increase. Detailed modeling and scoping of NPA for the OPTEMIST beamline are left to future works.

Fast ion losses to the first wall in W7-X provide a clean measurement of changes in fast ion confinement but highlight the three-dimensional nature of fast ion loss patterns in stellarators (Fig. 13). As plasma beta increases, we find loss regions where fast ion loads to the first wall decrease, regions where fast ion loads increase, and regions where loads shift. We see a region in the lower left of the figure where

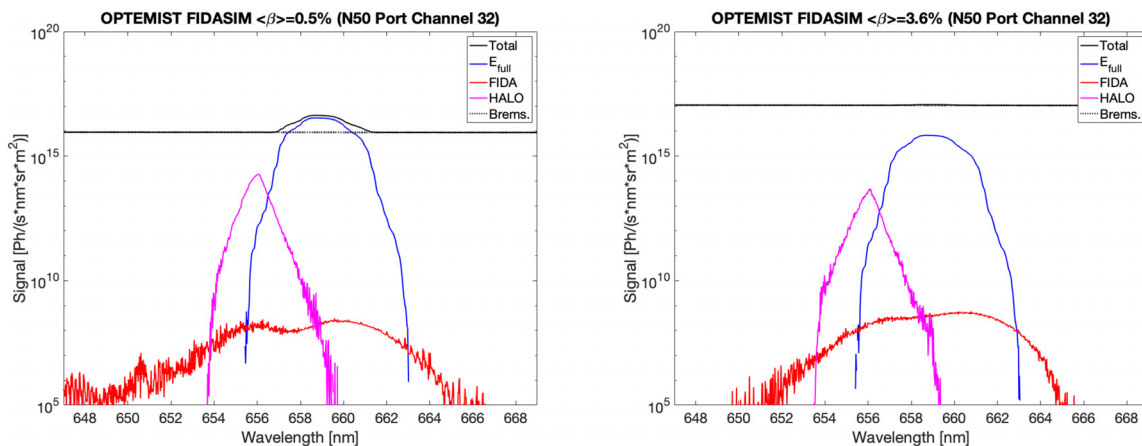


FIG. 12. Simulated FIDA spectrum for low beta (left) and high beta (right) signals from the monoenergetic 120 keV OPTEMIST beamline. The total signal is dominated by bremsstrahlung making the measurement nearly impossible.

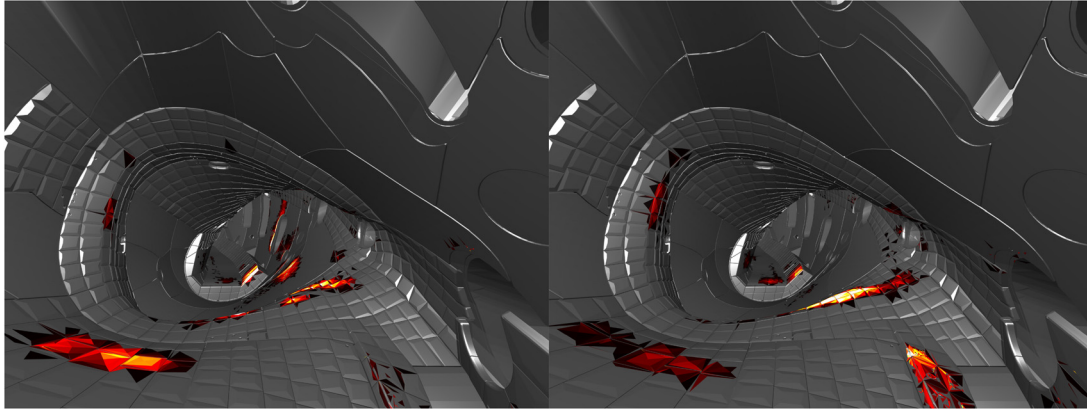


FIG. 13. Simulated fast ion wall loads for the low beta (left) and high beta (right) 120 keV beamline runs. Color threshold has been chosen to go from 0 to 1 MW/m² per megawatt injected.

loads decrease as plasma beta increases. Additionally, a large load on the smooth steel panel completely disappears. Loads on the inboard side of the triangular cross section show a poloidal shift upward. Finally, we find an increase in loads to the protective “bump” in the triangular cross section along with an increase to those going to the high iota baffle (lower right). This varied and dynamic load pattern implies that single point measurements are not sufficient for assessing the change in fast ion confinement.

Two sets of tiles were selected as candidate FC-FILD sensor locations and their signal modeled for changes in plasma beta (Fig. 14). The FC-FILD sensors are energy discriminating sensors that can be mounted inside wall tiles due to their small form factor and high heat tolerance. Prototype sensors have already been manufactured and demonstrated in W7-X, validating the in-tile mounting scheme.^{21,26} In this analysis, the monoenergetic 120 keV particle flux to the wall triangles (colored in red) was binned by sensor, then scaled from the total triangle area to a slit 40 × 5 mm². This is the size of the slit in the W7-X prototype diagnostic. In this analysis, a 1 MW (neutralized) beam at

120 keV was assumed so the signal level can also be read as A/MW (here 1 MW is approximately 8 A of current). All signal levels are well above the demonstrated sensitivity of such sensors in W7-X.

From the data traces, it is clear that some sensors see a continual decrease in signal with increasing plasma beta while others can show a more complex dependency. This behavior highlights the need for multi-point measurements. Sensor 8 sees a continual decrease in signal with plasma beta. However, no signal is present for the highest beta case. Sensor 15 shows a continual increase in signal with plasma beta but no signal at the lowest plasma beta case. Examining an ensemble of sensors, we see that array 1 (sensors 1–8) shows a decrease in overall signal with plasma beta. Meanwhile, array 2 (sensors 9–16) shows a relatively constant signal with plasma beta. This highlights the complex nature of wall loads with plasma beta and the necessity for multi-point measurements. A more detailed analysis including energy spectra is left to future work, here we simply show that with a modest set of FC-FILD sensors the improvement in confinement with plasma beta can be measured.

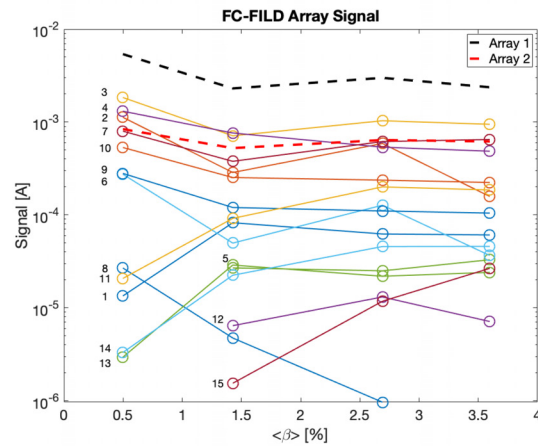
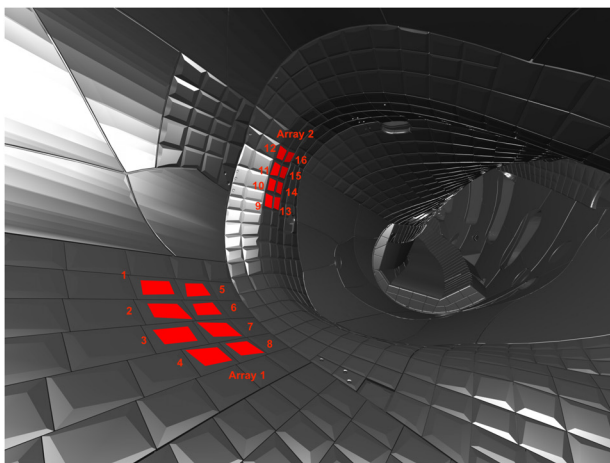


FIG. 14. FC-FILD sensor locations (left) and signals as a function of plasma beta (right). Sensors have been numbered in both plots, with array 1 referring to sensors 1–8 and array 2 referring to sensors 9–16. An aperture size of 40 × 5 mm² has been assumed for the diagnostic in each tile.

24 July 2024 06:56:36

IV. DISCUSSION

In this work, the ability of the existing neutral beam system, D–D fusion produced fast tritons, and a purpose built probing neutral beam to measure the optimization of drift orbits was explored. It was found that the geometry of the existing neutral beam system is insufficient to generate the necessary collisionless trapped particles needed to assess this characteristic of W7-X. This is attributed to the strong toroidal variation in the magnetic field, resulting in the neutral beams generating passing particles by injecting into a high field region, despite nearly radial injection. Fast tritons as generated by D–D fusion reactions were found to be able to generate deeply trapped collisionless particles but discrimination of these particles from the passing population would prove difficult. Additionally, the source term was a strong function of density (hence plasma beta), making birth measurement critical to assessing changes in fast ion confinement. Finally, the purpose built neutral beam, OPTEMIST, was explored using a more favorable injection geometry for the generation of trapped particles. High levels of bremsstrahlung due to high plasma densities were found to preclude the use of FIDA, but fast ion losses clearly changed with increasing plasma beta, demonstrating the desired effect. In the end, this work found the OPTEMIST beam at 120 kV would provide the most straightforward confirmation of the closing of poloidal drift orbits in W7-X.

While the existing neutral beam system was not found to produce the necessary particles, this study does highlight some interesting features of quasi-omnigeneous configuration that approach a quasi-poloidal symmetry. In such devices, deeply trapped particles can only be born in the toroidal regions of low field. Additionally, this work highlights that, even then, a small amount of parallel velocity results in particles that are not deeply trapped. This implies that such stellarator configurations may be able to reduce the overall phase space volume where trapped particles can be born. This is because the width of the variation of magnetic field strength toroidally can be minimized. Such configurations have already been realized in the W7-X device, the so-called narrow mirror magnetic configuration. It would appear that when designing future reactors, one could not only improve the confinement of trapped alphas through drift orbit optimization but also minimize the phase-space volume where deeply trapped particles can exist.

The OPTEMIST beam proposed in this paper is a 120 kV monoenergetic proton beam, which is not a traditional neutral beam. Traditionally, hydrogen neutral beams produce three energies due to the formation of hydrogen molecules in the ion source. Additionally, neutralization efficiency tends to drop with increasing beam energy. As a result, a traditional 120 kV beam would be biased toward the 60 and 40 kV beam energies. Such biasing would make discrimination of the 120 keV population difficult. While beyond the scope of this work, a possible path forward is proposed through a novel neutral beam design. Here, instead of bending away the un-neutralized ion beam components after neutralization using a magnetic field, as is done in a traditional neutral beam, we propose bending the beam before neutralization. In this way, the 120 keV ions would be the only ones to pass through the neutralizer and a monoenergetic beam would be formed. Moreover, the unionized 120 kV ion beam could be bent back through the neutralizer. This could create a multi-pass neutralizer that, in theory, could drastically increase the neutralization efficiency of the high energy beam. This would also avoid the need for a negative ion beam,

which comes with its own set of challenges. Assessment of such a beam design is left to future work.

ACKNOWLEDGMENTS

This work has been carried out within the framework of the EUROfusion Consortium, funded by the European Union via the Euratom Research and Training Programme (Grant Agreement No 101052200—EUROfusion). Views and opinions expressed are however those of the author(s) only and do not necessarily reflect those of the European Union or the European Commission. Neither the European Union nor the European Commission can be held responsible for them. Simulations were performed at the Max-Planck Computing and Data Facility on the Raven cluster. BEAMS3D runs were performed with v3.00 of the code, “develop” branch, hash af17e3acdd95b75ccb706bbaacddb444236dde0a.

AUTHOR DECLARATIONS

Conflict of Interest

The authors have no conflicts to disclose.

Author Contributions

Samuel A. Lazerson: Conceptualization (lead); Data curation (lead); Formal analysis (lead); Funding acquisition (lead); Investigation (lead); Methodology (lead); Software (lead); Validation (lead); Visualization (lead); Writing – original draft (lead); Writing – review & editing (lead). **David Kulla:** Conceptualization (supporting); Formal analysis (supporting); Investigation (equal); Methodology (equal); Software (supporting); Visualization (supporting); Writing – review & editing (supporting). **Paul McNeely:** Conceptualization (supporting); Methodology (supporting); Writing – review & editing (supporting). **Norbert Rust:** Conceptualization (supporting); Methodology (supporting); Writing – review & editing (supporting). **Lucas van Ham:** Conceptualization (supporting); Methodology (supporting); Writing – review & editing (supporting). **Dirk Hartmann:** Conceptualization (supporting); Methodology (supporting); Writing – review & editing (supporting).

DATA AVAILABILITY

The data that support the findings of this study are available from the corresponding author upon reasonable request.

REFERENCES

- ¹W. Lotz, P. Merkel, J. Nührenberg, and E. Strumberger, *Plasma Phys. Controlled Fusion* **34**, 1037 (1992).
- ²P. J. Catto, *Phys. Fluids* **24**, 1663 (1981).
- ³D. A. Spong, S. P. Hirshman, J. C. Whitson, D. B. Batchelor, B. A. Carreras, V. E. Lynch, and J. A. Rome, *Phys. Plasmas* **5**, 1752 (1998).
- ⁴J. Faustin, W. Cooper, J. Graves, D. Pfefferlé, and J. Geiger, *Nucl. Fusion* **56**, 092006 (2016).
- ⁵C. Slaby, S. Äkäslompolo, M. Borchardt, J. Geiger, R. Kleiber, A. Könies, S. Bozhenkov, C. Brandt, A. Dinklage, M. Dreval, O. Ford, G. Fuchert, D. Hartmann, M. Hirsch, U. Höfel, Z. Huang, P. McNeely, N. Pablant, K. Rahbarnia, N. Rust, J. Schilling, A. von Stechow, H. Thomsen, and Wendelstein 7-X team, *Nucl. Fusion* **60**, 112004 (2020).
- ⁶S. A. Lazerson, O. Ford, S. Äkäslompolo, S. Bozhenkov, C. Slaby, L. Vanó, A. Spanier, P. McNeely, N. Rust, D. Hartmann, P. Poloskei, B. Buttenschon,

- R. Burhenn, N. Tamura, R. Bussiahn, T. Wegner, M. Drevlak, Y. Turkin, K. Ogawa, J. Knauer, K. J. Brunner, E. Pasch, M. Beurskens, H. Damm, G. Fuchert, P. Nelde, E. Scott, N. Pablant, A. Langenberg, P. Traverso, P. Valson, U. Hergenbahn, A. Pavone, K. Rahbarnia, T. Andreeva, J. Schilling, C. Brandt, U. Neuner, H. Thomsen, N. Chaudhary, U. Höefel, T. Stange, G. Weir, N. Marushchenko, M. Jakubowski, A. Ali, Y. Gao, H. Niemann, A. Puig Sitjes, R. Koenig, R. Schroeder, N. den Harder, B. Heinemann, C. Hopf, R. Riedl, R. C. Wolf, and W7-X Team, *Nucl. Fusion* **61**, 096008 (2021).
- ⁷J. Ongena, A. Messiaen, Y. Kazakov, B. Schweer, I. Stepanov, M. Vervier, K. Crombé, M. V. Schoor, V. Borsuk, D. Castaño-Bardawil, A. Kraemer-Flecken, K. P. Hollfeld, G. Offermanns, D. A. Hartmann, J. P. Kallmeyer, and R. C. Wolf, *AIP Conf. Proc.* **2254**, 070003 (2020).
- ⁸D. Kulla, S. Lazerson, S. Günter, M. Hirsch, D. Hartmann, P. McNeely, N. Rust, and R. C. Wolf, *Plasma Phys. Controlled Fusion* **64**, 035006 (2022).
- ⁹J. M. Faustin, J. P. Graves, W. A. Cooper, S. Lanthaler, L. Villard, D. Pfefferlé, J. Geiger, Y. O. Kazakov, and D. V. Eester, *Plasma Phys. Controlled Fusion* **59**, 084001 (2017).
- ¹⁰W. W. Heidbrink, D. Liu, Y. Luo, E. Ruskov, and B. Geiger, *Commun. Comput. Phys.* **10**, 716 (2011).
- ¹¹M. McMillan and S. A. Lazerson, *Plasma Phys. Controlled Fusion* **56**, 095019 (2014).
- ¹²S. A. Lazerson, D. Kulla, D. A. Hartmann, P. McNeely, N. Rust, and W7-X Team *Nucl. Fusion* **63**, 096012 (2023).
- ¹³S. K. Seal, S. P. Hirshman, A. Wingen, R. S. Wilcox, M. R. Cianciosa, and E. A. Unterberg *2016 45th International Conference on Parallel Processing (ICPP)* (IEEE, Philadelphia, PA, 2016), pp. 618–627.
- ¹⁴D. Kulla, “Validation of BEAMS3D against ASDEX upgrade data using FIDASIM,” (unpublished).
- ¹⁵S. Suzuki, T. Shirai, M. Nemoto, K. Tobita, H. Kubo, T. Sugie, A. Sakasai, and Y. Kusama, *Plasma Phys. Controlled Fusion* **40**, 2097 (1998).
- ¹⁶S. A. Lazerson, O. P. Ford, C. Nuehrenberg, S. Äkäsloppolo, P. Z. Poloskei, M. Machiels, P. McNeely, L. Vanó, N. Rust, S. Bozhenkov, T. W. Neelis, J. P. Graves, D. Pfefferlé, A. Spanier, D. Hartmann, N. Marushchenko, Y. Turkin, M. Hirsch, N. Chaudhary, U. Hoefel, T. Stange, G. Weir, N. Pablant, A. Langenberg, P. Traverso, P. Valson, J. Knauer, K. Jakob Brunner, E. Pasch, M. Beurskens, H. Damm, G. Fuchert, P. Nelde, E. Scott, U. Hergenbahn, A. Pavone, K. Rahbarnia, T. Andreeva, J. Schilling, C. Brandt, U. Neuner, H. Thomsen, M. Jakubowski, A. Ali, Y. Gao, H. Niemann, A. Puig Sitjes, R. Koenig, R. C. Wolf, and W7-X Team. *Nucl. Fusion* **60**, 076020 (2020).
- ¹⁷H.-S. Bosch and G. Hale, *Nucl. Fusion* **32**, 611 (1992).
- ¹⁸S. A. Lazerson, A. LeViness, and J. Lion, *Plasma Phys. Controlled Fusion* **63**, 125033 (2021b).
- ¹⁹S. A. Lazerson, D. Pfefferlé, M. Drevlak, H. Smith, J. Geiger, S. Äkäsloppolo, P. Xanthopoulos, A. Dinklage, O. Ford, P. McNeely, N. Rust, S. Bozhenkov, D. Hartmann, K. Rahbarnia, T. Andreeva, J. Schilling, C. Brandt, U. Neuner, H. Thomsen, R. C. Wolf, and W7-X Team. *Nucl. Fusion* **61**, 096005 (2021).
- ²⁰S. A. Lazerson, R. Ellis, C. Freeman, J. Ilagan, T. Wang, L. Shao, N. Allen, D. Gates, and H. Neilson, *Rev. Sci. Instrum.* **90**, 093504 (2019).
- ²¹D. Kulla, S. A. Lazerson, K. Hunger, H. Gerdes, and R. Bandorf, *Rev. Sci. Instrum.* **94**, 053503 (2023).
- ²²W. I. van Rij and S. P. Hirshman, *Phys. Fluids BPhys.* **1**, 563 (1989).
- ²³J. Kontula, J. P. Koschinsky, S. Äkäsloppolo, and T. Kurki-Suonio, *Plasma Phys. Controlled Fusion* **63**, 035022 (2021).
- ²⁴H. Nuga, R. Seki, K. Ogawa, H. Yamaguchi, S. Kamio, Y. Fujiwara, Y. Kawamoto, M. Yoshinuma, T. Kobayashi, Y. Takemura, M. Isobe, M. Osakabe, and M. Yokoyama, *Nucl. Fusion* **64**, 066001 (2024).
- ²⁵S. Bannmann, S. Bozhenkov, S. Äkäsloppolo, P. Poloskei, W. Schneider, O. Ford, and R. Wolf, *J. Instrumentation* **17**, P01034 (2022).
- ²⁶S. A. Lazerson, D. Kulla, A. LeViness, M. Steffen, B. Kursinski, and K. Ewert, “First measurements with the Faraday cup fast ion loss detector on Wendelstein 7-X,” *Rev. Sci. Instrum.* (submitted).